Springer

KSME

Journal of Mechanical Science and Technology 25 (8) (2011) 1949~1960
www.springerlink.com/content/1738-494x
DOI 10.1007/s12206-011-0604-8

Three-dimensional flow characteristics of propeller-propulsion WIG effect vehicle with direct underside pressurization †

Juhee Lee[1], Byung Moon Kim[2] and Kyoungwoo Park[3,*]

[1]*Mechatronics Engineering, Hoseo University, Asan 336-795, Korea*
[2]*College of Energy & Environment, Dongguk University, Gyungju 708-714, Korea*
[3]*Faculty of Engineering, Department of Mechanical Engineering, Hoseo University, Asan 336-795, Korea*

(Manuscript Received January 4, 2011; Revised May 16, 2011; Accepted June 2, 2011)

Abstract

Numerical investigations for a 3-dimensional WIG effect vehicle with DUP (direct underside pressurization) have been performed. The purpose of this study is to analyze the aerodynamic characteristics and static height stability of DUP using computational fluid dynamics (CFD). When a WIG effect vehicle accelerates to take off on water, increased pressure under the fuselage by DUP (propeller and air chamber) can considerably reduce the take-off speed and thus minimize the effect of the hump drag which is one of the technical difficulties of a WIG effect vehicle. The accelerated air by the propeller enters the air chamber through a channel in the middle of the fuselage resulting in an augmentation of the lift by changing the air pressure from dynamic to static. However, the DUP is not favorable for both stability and aerodynamic performance of the WIG effect vehicle because the accelerated air produces an excessive drag, negative pitching moment and 3-dimensional effects (that is, yawing and rolling moments). The result shows that the effect of yawing and rolling moments is not serious.

Keywords: Aerodynamic characteristics; CFD (computational fluid dynamics); DUP (direct underside pressurization); Ground effect; WIG (wing-in-ground) effect vehicle; Yawing moment, Rolling moment

1. Introduction

The wing-in-ground (WIG) effect vehicle is an advanced vehicle that cruises close to water or ground surface (i.e., at a height of 30% or less of its chord length) by utilizing an air cushion between the wing, the fuselage and the ground. Due to the air cushion at low heights, there is a considerable increase in lift with a decrease in drag, and therefore enhancement of the lift–drag ratio [1-5]. The enhancement of the lift-drag ratio makes the WIG effect vehicle a potential means of transportation. That is, the WIG effect vehicle can be an alternative means of next-generation transportation in the near future, occupying the niche between ships and aircraft. Neither the speed of a fast ship nor the efficiency of an economical aircraft can be better than that of the WIG effect vehicle. However, there are a few technical difficulties in cramping the progress of the potential WIG effect vehicle; hump drag [6], static height stability [7], etc.

The von Karman-Gabriell's diagram [8] depicts the efficiency of various modes of transportation in a single picture. A remarkable thing to note in the diagram is the triangular area at the center of the technology line where no conventional means of transportation appears. The WIG effect craft, a flying ship cruising with the speed of 100 to 400 km/h and lift-to-drag ratios of 15 to 30, can fill the speed and efficiency gap between the marine and air transports. In general, the lift and drag forces of a wing will change considerably near the ground. These phenomena during the takeoff and landing have been observed by several studies [1-3, 9] from as early as the 1900s. According to their results, the ground has a great influence (suction and stagnation) on the pressure distributions along the wing surface. Oncoming air to the lower wing surface gradually decreases the magnitude of the speed of the aircraft and changes to static pressure. This eventual increase of pressure is called an air cushion or a ram effect.

In 1922, Wieselsberger [1] performed a theoretical investigation to determine the conditions for taking off and landing of an airplane using Prandtl's wing theory. He utilized the image method and replaced the surface of the ground by a second wing at the same distance but on the opposite side. The reduction in the induced drag of a monoplane and a multiplane in ground effect was estimated in terms of the ground clearance, the aspect ratio, and the lift coefficient. The theoretical predictions agreed well with the experimental results. Wie-

† This paper was recommended for publication in revised form by Associate Editor Do Hyung Lee

* Corresponding author. Tel.: +82 41 540 5804, Fax.: +82 41 540 5808
E-mail address: kpark@hoseo.edu

selsberger noted that a longer runway for a landing was necessary because of an excessive lift due to this air cushion. The pressure distributions on the lower surface became somewhat constant and the strength of the pressure increased with the ground proximity caused by the air cushion. On the other hand, the pressure distributions on the upper surface varied with the suction and wing profile.

For the wing in ground effect, generally, the pressure rise on its lower surface is considerably high so that the resultant force leads to an increase in lift. For finite wings in ground effect, the induced drag is decreased because of the decreased influence of the wing tip vortex. On the contrary, the center of the pitching moment tends to move to the mid chord where it is behind the center of gravity. The stability of the wings in ground effect also changes according to the center of the pitching moment.

The stability characteristics play an important role in designing a safe and efficient WIG effect vehicle due to its potential danger in ground effect. Staufenbiel and Schlichting [10] insisted that the static height stability is a part of the dynamic stability as well as a necessary condition for the stability. It means that the dynamic stability cannot be satisfied without the static height stability. Staufenbiel [11] studied the static height stability for the WIG effect vehicle and also found the nonlinearity by ground effect. He noted that the dangers of ground contact and heavy oscillations were disadvantages of applying an elevator as a primary longitudinal control, but thrust control was a favorable means of the height controls. This would be a good guideline for designing a control system for the WIG effect vehicle. Kornev and Matveev [12] performed an analysis of the static height stability using vortex lattice methods (VLM). In their study, there were three important factors for static height stability: tail unit, profiles of wing sections, and main wing profile. The static height stability for the WIG effect vehicle could not be satisfied by moving the center of gravity. The favorable range of the height stability for stable flight in ground effect was between -0.15 and -0.05. When the static height stability was less than -0.15, it became excessive and led to dynamic instability. In addition, when the static height stability was between 0 and -0.05, there was insufficient stability and led to long-period instability. For stable flight, they insisted that the center of gravity should be located between the aerodynamic centers of altitude and pitch and, furthermore, the close location to the center of altitude was favorable.

Aerodynamic transition characteristics of a power-augmented ram wing (PARWIG) for in-ground and out-of-ground effect cases were studied experimentally by Thomas et al. in 1979 [13]. They showed that the flap deflection and thrust coefficient variations provided the best method for flight-path control, and high nacelle deflections were useful in reducing the pitching-moment trim requirement for the vehicle, especially at high thrust coefficients. However, there was a thrust loss when the efflux was trapped under the wing which reduced the effective thrust available for acceleration by about a third of the installed thrust-to-weight ratio.

The vehicle in ground effect also required a proper control system for flight steadily skimming the water or ground surface. Majji et al. [14] performed an investigation on the dynamics and control of a ground effect vehicle. Mathematical models of the dynamics of a vehicle were presented and the inherent stability of the concept was evaluated through a numerical simulation. They insisted that Weisselsberger's model showed the self stabilization effect in the form of an aerodynamic spring, stabilizing the height for certain vehicle velocities.

Because the vehicle in ground effect skims the surface, its cruise performance is generally improved. However, the vehicle requires about double the engine power to obtain sufficient thrust during both takeoff and landing since part of the fuselage is sunk in water. In order to obtain the additional thrust, the engines take on an increase in drag, which gives rise to the structural problem of supporting the heavy engines in cruise [15]. In order to overcome the above mentioned problem in WIG effect vehicles, various devices have been developed [7]: aerodynamic high-lift devices generally used in an airplane, hydrodynamic high-lift devices such as hydro-ski or hydrofoil, and under side pressurization (DUP) such as air cushion or power augmentation (PAR). Among them, the DUP, which injects the exhaust of the jet engine or propeller to the underbody, improves lift by air cushion. Thus, it can lift up the vehicle at a lower takeoff speed. Recently, Park et al. [16] performed a numerical study on the aerodynamics of the WIG vehicle with the DUP. They predicted the aerodynamic forces and static height stability with assumption of a symmetric vehicle ignoring yawing and rolling moment. More recently, Lee et al. [17] performed an investigation of the same vehicle but did not show aerodynamic characteristics in detail.

The DUP can considerably improve the ability to take-off at a low speed and reduce the power mismatch between take-off and cruise. However, the additional lift due to DUP provides pressure drag instead of hump drag. The effect of DUP's heavy utilization of lift during take-off has not been commonly recognized in previous studies. A detailed aerodynamic investigation on the DUP of a WIG effect vehicle is required. In the present study, the three-dimensional flow characteristics and the height static stability of WIG effect vehicle with DUP that consists of all compartments such as fuselage, wings, DUP and T-tail are investigated numerically. Numerical analyses are performed by solving the Reynolds-Averaged Navier-Stokes (RANS) of turbulent flow. The aerodynamic characteristics are obtained and compared for various conditions such as pitch angles and non-dimensional heights.

2. Computational models and validation

2.1 Computational models

Air is taken as the working fluid and is assumed to be steady, incompressible, and have turbulent flow. The fluid properties are taken to be constant and the effect of viscous dissipation is assumed to be negligibly small. Using the aforementioned assumptions, the Reynolds-Averaged Navier-Stokes (RANS) equations for mass and momentum, which are

written in a tensor notation, have to be solved.

$$\frac{\partial(\rho u_j)}{\partial x_j} = 0 \tag{1}$$

$$\frac{\partial(\rho u_i u_j)}{\partial x_j} = -\frac{\partial P}{\partial x_i} + \frac{\partial}{\partial x_j}\left[\mu\left(\frac{\partial u_i}{\partial x_j} + \frac{\partial u_j}{\partial u_i}\right) - \overline{\rho u_i' u_j'}\right] \tag{2}$$

The new term, $\overline{\rho u_i' u_j'}$, the Reynolds stress, must be modeled by using a turbulence model in order to solve the RANS equations. In this study, the flow domain was divided into two regions such as near wall and fully turbulent regions, and then adopted a standard turbulent model [18] and wall function next to the wall. According to this model, turbulent kinetic energy (k) and its dissipation rate (ε) are expressed in a tensor form as follows:

$$\frac{\partial}{\partial x_j}\left(\rho u_i k\right) = \frac{\partial}{\partial x_j}\left[\frac{\mu_t}{\sigma_k}\frac{\partial k}{\partial x_j}\right] + P_k - \rho\varepsilon \tag{3}$$

$$\varepsilon = \frac{k^{3/2}}{l_\varepsilon}\left(1 + \frac{C_\varepsilon}{\mathrm{Re}_y}\right) \tag{4}$$

where i = 1, 2 and 3 denote the x, y, and z-directions, respectively. The term P_k in Eq. (3) stands for the production term. The model constants and various functions used in the turbulent model are detailed in Ref. [18].

The numerical simulations presented in this work were done by means of STAR-CCM+ [19] which is a general purpose commercial software. The pressure-velocity coupling phenomenon is resolved through the SIMPLE algorithm [20]. For representing the exact flight conditions, the moving wall boundary condition with a flight velocity is applied at the ground. The solutions are treated as converged ones when the sum of normalized residual is less than 1×10^{-5}. A fan performance curve for the propeller was not available. Thus, a propeller can be re-built by reverse engineering and the computational experiments are performed with a propeller alone to obtain propeller performance (pressure vs. mass flow rate). The flow analysis for the WIG effect vehicle is carried out by the moment source method instead of a real propeller conditions.

2.2 Validation of CFD models

To validate the present CFD model, the experiment [21] and analytical results [22, 23] for lift and drag coefficients are plotted in Fig. 1. For this, a rectangular wing of the untwisted NACA 0015 profile (i.e., aspect ratio of 6.6) with Reynolds number of 1.5×10^6 is used. The 3-dimensional shaped wing is placed far away from the ground (that is, ground effect is neg ligible). As can be seen in Fig. 1, the computational results have a little discrepancy compared to those of experiments. This is due to the fact that the measurement data were listed without proper corrections for the blockage factor and lift interference, as the authors mentioned in their paper. It is also shown that the results of this study are in good agreement with the analytic solutions.

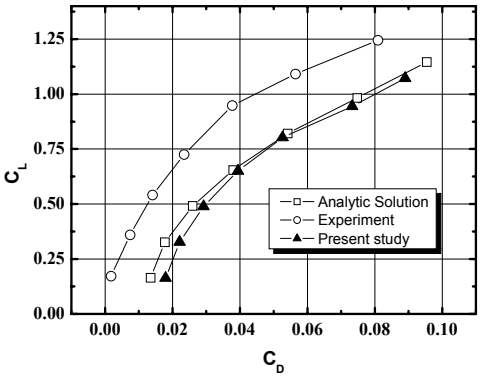

Fig. 1. Comparision of drag polars; analytic solution [22], experiment [21] and present method.

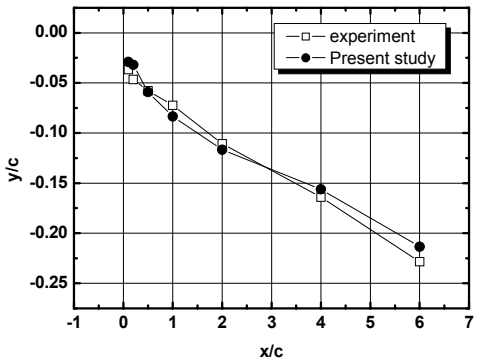

(a) Wing tip vortex location along y-coordinate (outward from trailing edge at wing tip)

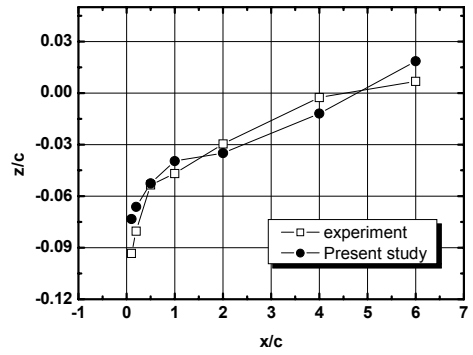

(b) Wing tip vortex location along z-coordinate (upward from trailing edge at wing tip)

Fig. 2. Comarision of wing tip vortex location; experiment [21] and present method.

The computational trajectories of the wing tip vortex are also compared with the experiments and they are presented in Fig. 2. Fig. 2 indicates very small deviations from the measurements in the calculated wing tip vortex locations. The comparison results show that the CFD model employed in this study can be analyze the flow characteristics of propeller-propulsion WIG effect vehicle.

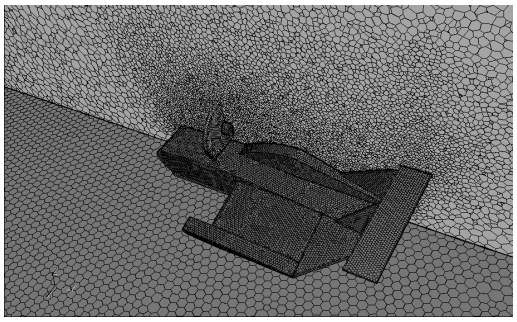

(a) Non-uniformly distributed grid system aroud the vehicle

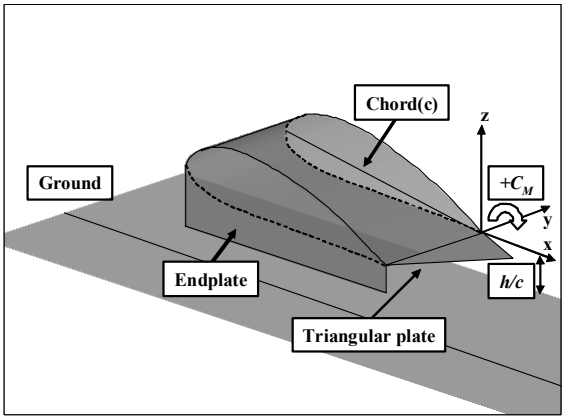

(b) Definition of height and compartments of vehicle

Fig. 3. Computational grid system and geometry.

3. Results and discussion

The computational domain considered in this study is extended 6 times of a vehicle length for each direction in order to avoid the influence of the far boundaries, but it is extended 10 times for the downstream direction. To take the no-slip boundary condition on the surface into account correctly, 6 layers of the prism grid with high aspect ratio along the surface are used next to the surface. To evaluate the forces on the vehicle surface, locally refined grids next to the vehicle are employed. The grid system and the computational domain are shown in Fig. 3. The non-dimensional height between the wing and the ground is measured at the trailing edge, and the nose-up pitching moment is positive, as shown in Fig. 3(b). The numerical calculations are performed from $h/c = 0.24$ to 0.45 and $\alpha = -2^o$ to 10 degrees except at $h/c = 0.24$ and $\alpha = -2^o$ due to the fuselage's contact with the ground. To investigate grid dependency, three different numbers of grids are tested by comparing the C_L and C_D in the case of $\alpha = 0^o$, h/c = 0.24, and v_{in} = 10 *m/s* with DUP ; 740,000 (coarse), 980,000 (base) and 1,330,000 (fine). The results obtained from the three grid systems are 6.42, 6.08, and 6.11 for C_L and 5.07, 4.42, and 4.39 for C_D, respectively. For example, the relative error between base and fine grids for C_L is 0.5%, while that between the base and coarse grids are estimated as 5.6%. From these results and considering the computational cost, all computational results are obtained from the base grid system in the present work.

Table 1. Boundary conditions.

Inlet	Uniform velocity
Outlet	Pressure
Ground	Moving wall
Vehicle surface	Non-slip wall
Others (far boundaries)	Slip wall

Table 2. Specifications of model vehicle.

Maximum speed	About 25 m/s (72 km/h)
Cruise speed	15 m/s (54 km/h)
Engine power	1 ps at 10000 rpm
Propeller diameter	24 cm (9.5 $inch$)
Main wing area	0.10976 m^2
Tail wing area	0.07558 m^2
Control surface	Rudder
Total weight	About 2.7 kg
Total length	1 m
Span	0.7 m
Chord length	0.334 m
Taper ratio(including triangular plate)	0.75
Twisting angle	0 °

The boundary conditions are configured to identify the free-flight condition. The upstream boundary is modeled using an inlet velocity with a uniform distribution. A pressure outlet boundary condition is adopted at the downstream. A slip wall boundary condition is imposed on the undisturbed far boundary, thus imposing a zero cross flow condition. The wing and ground plane are modeled as solid walls with a no-slip boundary condition. In addition, the ground surface is provided with a velocity equal to free stream for identifying free flight through calm air (Table 1). The Reynolds numbers based on both free stream velocities (v_{in} = 10 and 15 m/s) and chord length of the vehicle are 2.14×10^5 and 3.21×10^5, respectively. The detail specifications of the model vehicle are listed in Table 2.

3.1 Aerodynamic characteristics and static height stability

Fig. 4 presents the flow streams along the center line of the vehicle for $\alpha = 9^o$ and $h/c = 0.24$ (i.e., the vehicle is close to the ground) in order to explain the overall flow pattern around the WIG vehicle. The accelerated air coming to the DUP flows along the surface of the fuselage with high dynamic pressure. It is also shown that a part of the accelerated air comes into the lower surface of the fuselage and runs through the small gap between the ground and wing, as shown in Fig. 4. There is another flow passage leading air into the air chamber, the fore gap between the fuselage and ground. From the figure, higher pressure on the aft body of the vehicle is ex-

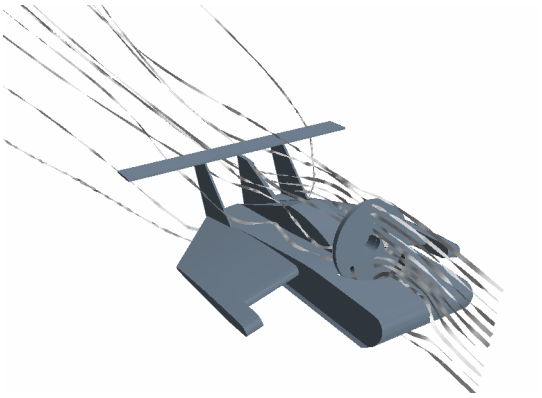

Fig. 4. 3-dimensional flow streams around the model vehicle.

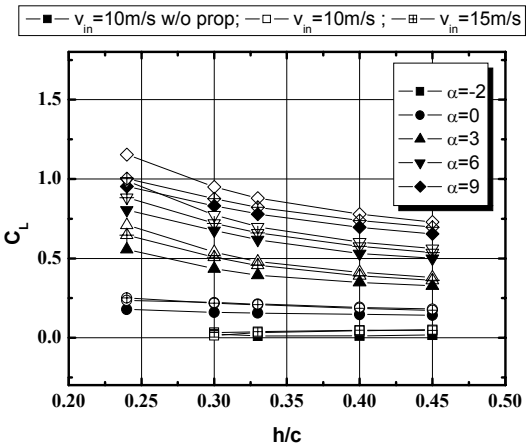

Fig. 5. Lift augmentatio of a vehicle in ground effect with and without DUP.

pected because of air stagnation in the air chamber. Note that this higher dynamic pressure can augment both the lift and drag forces and the pitching moment as the vehicle is approaching the ground.

In general, the ground effect improves the aerodynamic forces because of an increase in pressure on the lower surface and a decrease in the influence of the wing tip vortex. Fig. 5 shows the lift coefficients (C_L) as a function of dimensionless height (h/c) with and without DUPs. As shown in Fig. 5, except for the case of negative pitch angle ($\alpha = -2^o$), the lift coefficients of all cases (that is, $v_{in} = 10$ m/s without DUP, $v_{in} = 10$ m/s and $v_{in} = 15$ m/s with DUP) are increased as h/c decreases due to the ground effect. A larger pitch angle results in a higher increase in lift coefficient. This result, greater lift at lower height, agrees well with those of other research [5, 17, 24, 25]. It is also shown in Fig. 5 that for the same inlet velocity ($v_{in} = 10$ m/s) the lift force for the case of with DUP is higher than that without DUP. It implies that DUP has a great influence on lift augmentation. When the pitch angle is greater than 3^o, the lift coefficient for $v_{in} = 15$ m/s becomes smaller than that for $v_{in} = 10$ m/s since the pressure fraction by the DUP to the dynamic pressure is relatively small. It is interesting that all lift coefficients at $\alpha = -2^o$ decrease when the vehicle gets close to the ground and the cases with DUP have a larger decrease in lift coefficient at this pitch angle (to be discussed later). This result is mainly due to the shape of the front part of the fuselage, which results in the Venturi effect or diverge-converge effect between the fuselage and ground. It is also shown in Fig. 5 that C_L is linearly proportional to α at $h/c = 0.45$, but not at $h/c = 0.24$ where the effect of ground is stronger. The similar non-linear increase in lift can be seen in other researches. The non-linear increase is due to the fact that when the vehicle is in ground effect above the critical pitch angle (between -2^o to 0^o), the oncoming air through the DUP and leading edge is stagnant because of the small gap between fuselage and ground so that the pressure is suddenly increased. However, for cases outside of critical pitch angle and height, the increasing rate of pressure is slow and increases linearly as the general airplane does.

The aerodynamic characteristics of lift and drag can be wrapped into a single diagram; the drag polar. Virtually improving the aerodynamic performance of wings in ground effect can be achieved by increasing the lift and reducing the drag at the same time. Thus, a high performance airfoil or vehicles may be placed at the left in a drag polar diagram. The drag polar according to the heights for three cases are plotted in Fig. 6 and, in the present work, the total drag consists of zero-lift drag and drag due to lift. In general, the drag due to lift is reduced as the vehicle approaches the ground so that the aerodynamic efficiency, range, and endurance can be improved [23]. As shown in Fig. 6, the total drag for $v_{in} = 10$ m/s with DUP becomes the largest followed by $v_{in} = 15$ m/s (with DUP) and $v_{in} = 10$ m/s (without DUP). For the subsonic flow, the total drag of the WIG effect vehicle or generic airplane is comprised of three components such as form, friction, and induced drags. Fig. 6 shows that the zero-lift drag for $v_{in} = 10$ m/s with DUP has the largest value among three cases. This implies the negative effect of DUP on the dynamic pressure; increasing in the friction and form drags. Owing to the computational method, the friction drag can be easily separated from the total drag. Friction drag coefficients of $v_{in} = 10$ m/s, $v_{in} = 15$ m/s, and $v_{in} = 10$ m/s (without a propeller) at $h/c = 0.24$ and $\alpha = 0^o$ are calculated as 0.0227, 0.015, and 0.0122; the dimensional values (drag) are 0.61, 0.908 and 0.328. Although a complete list of the friction drag is not included, the same tendency can be observed for the entire drag. However, the drag for $v_{in} = 15$ m/s with DUP becomes lower because the rate of pressure rise by a propeller to dynamic pressure is low, and thus, its value is placed on the left compared to that of 10 m/s. The DUP by the augmented dynamic pressure increases lift and drag, simultaneously. As a result, the two cases with DUP are placed on the right side in Fig. 6, and thus, low operating performance is predicted. For the case of $h/c = 0.45$, the minimum drag is occurred at $C_L = 0$ whereas it appears at around $C_L = 0.25$ for $h/c = 0.24$. This implies that the vehicle obtains the minimum drag when it has a small pitch angle. The cruising vehicle in ground effect with

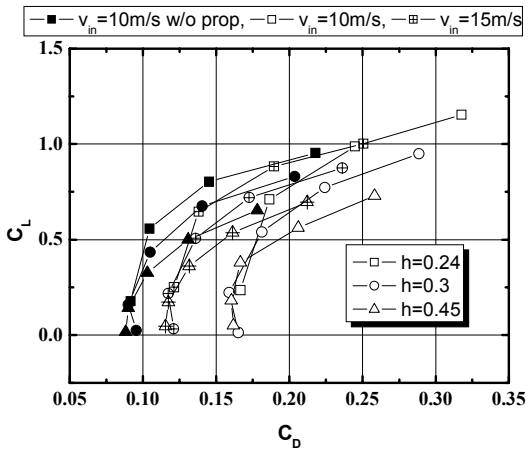

Fig. 6. Comparison of drag polars according to height.

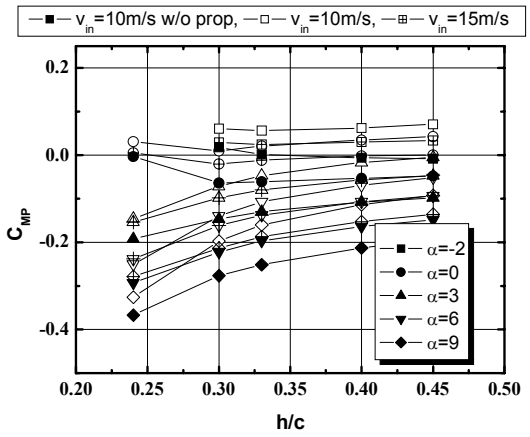

Fig. 7. Comparison of pitching moment according to pitching angles with and without DUP.

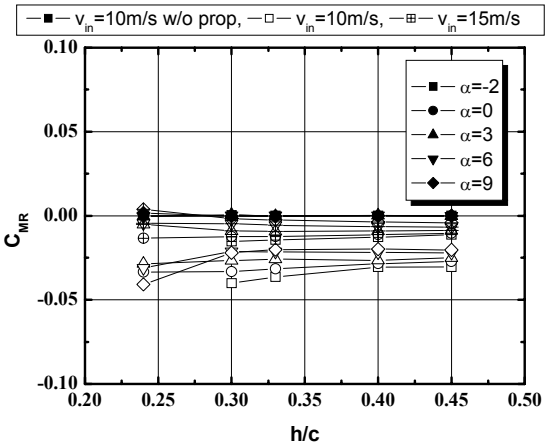

Fig. 8. Comparison of rolling moments according to pitching angle with and without DUP.

a small pitch angle obtains better operational efficiency.

Fig. 7 shows the effects of the height, incoming velocity, and pitching angle on the pitching moment (C_{MP}). The pitching moments are measured at a center of gravity and the nose-up pitching moment is defined as positive (+). It is easily found that the pitching moment is decreased and has negative values as the WIG craft approaches the ground with high α. It is well known that three significant factors, such as an air chamber, a horizontal tail, and a fore portion of the fuselage have an effect on the C_{MP} according to the height and pitching angle. The physical phenomena due to the three factors are explained as follows: (1) The stagnant air in the air chamber causes the high pressure at the aft of the fuselage and it leads to the negative moment against the center of gravity with decreasing height. Thus, the closer the vehicle approaches to the ground, the stronger the negative pitching moment gets. (2) The horizontal T-tail also generates the negative pitching moment with respect to the angle of attack. However, it has a marginal effect on the moment changes according to the height because it is placed sufficiently away from the ground; out of ground effect. It is also found from Fig. 7 that when the pitch angle is small ($\alpha < 3^o$), the C_{MP} is increased. This is due to the fact that the incoming air is not properly stagnated in the air chamber for both $h/c < 0.3$ and $\alpha < 3^o$ to decrease the pressure in the chamber, resulting in failure to produce the negative pitching moment. (3) The force on the front portion of the fuselage has a significant role in the moment since the arm of the moment is large. The presence of the ground causes the velocity of the air around the fore body of the fuselage to decrease on the lower surface and increase in pressure as the gap between the fore body and the ground becomes small. It is clear that the increase in pressure on the fore fuselage leads to the positive pitching moment. The pressure recovery on the lower surface of the fore body yields the positive pitching moment at $h/c = 0.3$ and $\alpha < 0^o$ as shown in Fig. 7. Moryseff and Levy [26], who studied the inversed wing in ground effect, showed an increase in pressure at the leading edge with an extremely low height of $h/c = 0.2$. The pressure increment at the leading edge with inversed wing was also observed by Zerihan and Zhang [27, 28] even though they did not clearly note this phenomenon. Additionally, from the point of static stability (*H.S.*) view, which is a necessary condition for dynamic stability and will be discussed later, it is important that the vehicle must have a negative pitching moment slope with respect to a pitching angle in order to satisfy the longitudinal stability [29]. Fig. 7 also shows that the pitching moment has a positive value at $\alpha = 0^o$ in order to trim the WIG vehicle at a positive pitching angle. If this is not so, the vehicle cannot maintain its height in the air such as in the case of without DUP. Only the case with DUP can be satisfied with the conditions because the model vehicle is designed to operate with DUP.

In order to explain the effect of various parameters on the rolling moment (C_{MR}) of the WIG vehicle, the variation of C_{MR} is displayed in Fig. 8. Note that the propeller rotates in a counterclockwise direction and then the resultant rolling moment with respect to the fixed axis has a negative value. As shown in Fig. 8, the absolute value of the rolling moment for two DUP cases is larger than that without DUP and also de-

creases with a decrease in height (h/c) and an increase in pitching angles. These imply that the vehicle experiences the counterclockwise rotational moment by the propeller of DUP. The air passing through DUP obtains a rotational component from the propeller and will be stagnated on the lower surface of the vehicle. As a result, the pressure distributions on the lower surface will become asymmetric and therefore the asymmetric pressure on the lower fuselage surface will produce the rolling moment. However, the case without DUP shows a near-zero rolling moment because of symmetric forces on the WIG vehicle. The constant rolling moment with heights for $v_{in} = 10$ m/s and 15 m/s can be observed at $\alpha = 3^o$ and 0^o, respectively. It is also found that the C_{MR} of $v_{in} = 10$ m/s suddenly decreases with height decrease at both $\alpha > 3^o$ and $h/c < 0.3$, whereas that of $v_{in} = 15$ m/s gradually increases under the same conditions. However, it is worthy to note that even though the vehicle has a rolling moment by asymmetric pressure distribution on the vehicle surface, the WIG effect vehicle considered in this study is inherently stable. Suppose that the vehicle suddenly experiences the roll by asymmetric forces and results in reducing a ground gap on the wing. The lift force on the wing with small gap will increase whereas the lift force on the other wing will decrease. As a result, the vehicle develops a counter rolling moment that tends to rotate the vehicle back toward its equilibrium and is statically stable in rolling [30]. The yawing moment, which is not plotted in this study, shows a similar trend with the rolling moment. The values of the C_{MR} for the cases of with DUP become large whereas those of the case without DUP constantly become zero. From the results, the rolling and yawing moments are not as significant as the pitching moment in the present work.

The aerodynamic forces of the vehicle in ground effect, which vary according to α and h/c, lead to a different stable condition from out of ground effect such as a general airplane. The static height stability (*H. S.*), a condition considered both α and h/c for the vehicle in ground effect, was proposed by Irodov [31]. Irodov derived this with a coordinate system that has an origin at a trailing edge. In this study, the same coordinate system was used for convenience. The *H.S.* includes the differentiations of lift coefficient and pitching moment coefficient against heights and pitching angle, and it is defined as follows:

$$\boldsymbol{H.S.} = \frac{\boldsymbol{C_{M,\alpha}}}{\boldsymbol{C_{L,\alpha}}} - \frac{\boldsymbol{C_{M,h}}}{\boldsymbol{C_{L,h}}} = \boldsymbol{X_\alpha} - \boldsymbol{X_h} \le 0 \tag{5}$$

where the subscripts h and α in the moment and the lift coefficients represent the derivative of height and pitching angle, respectively. Eq. (5) implies that the aerodynamic center of height (X_h) should be placed upstream of the center of the pitch angle (X_a) in order to maintain the stability of the vehicle in ground effect.

Fig. 9 shows the static height stability of three cases with various angles of attack. *H. S.* in Fig. 9 shows that the case with

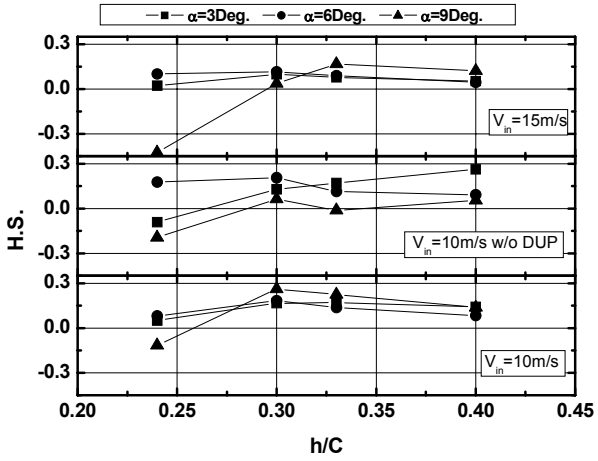

Fig. 9. Comparison of static height stability.

DUP is less stable than that without DUP when the vehicle is in ground effect. The pressure on the aft-portion of the air chamber for the case with DUP is increased as the height approaches the ground, resulting in high pressure that contributes to moving X_h downward. Thus the DUP is not favorable for H.S. However, in the case of $v_{in} = 10$ m/s and $\alpha = 9$ deg., the pressure on the air chamber and the lift on the T-tail increases with the patch angles, and therefore $C_{M,a}$ in Eq. (5) decreases so that X_a moves further downstream, improving stability as shown in Fig. 9. Fig. 9 shows that the vehicle has suddenly stopped its cruising height, which might be a cause of the overturn.

In terms of improving static height stability, it is possible to decrease $C_{M,\alpha}$ or increase $C_{M,h}$ as shown in Eq. (5). Two alternative ways to improve $C_{M,h}$ are possible: using a large tail to increase tail volume and moving a tail backward to have a large moment arm. The alternative way to improve the static height stability is changing X_h which has a no explicit relationship with a tail configuration but has a relationship with the fuselage and main wings. However, it is difficult to improve the static height stability because modification of the fuselage and wing shapes (such as S-shape profile) is required. Thus, a WIG effect vehicle generally employs a large T-tail to increase static height stability and the large T-tail has been one of the features of the WIG effect vehicles [7, 8].

3.2 Pressure distributions along the center of fuselage

Aerodynamic characteristics of WIG effect vehicles are significantly changed compared to those of airplanes due to the presence of ground and DUP. In this section, they are explained through the pressure distribution on the lower and upper surfaces of the model considered in this study.

Fig. 10 plots the pressure distributions (C_p) along the center of the body to show the effects of DUP and pitch angle on aerodynamic forces at $v_{in} = 10$ m/s and $h/c = 0.24$. It can be seen in Fig. 10(a) that for the case of with DUP(-■-), the pressure distribution on the upper surface is considerably different from that without DUP(-□-) due to differing dynamic pressure. This

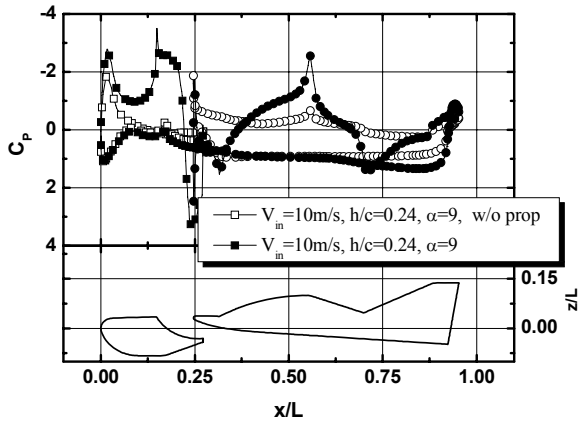

(a) C_P at high pitch angle ; $\alpha = 9^o$

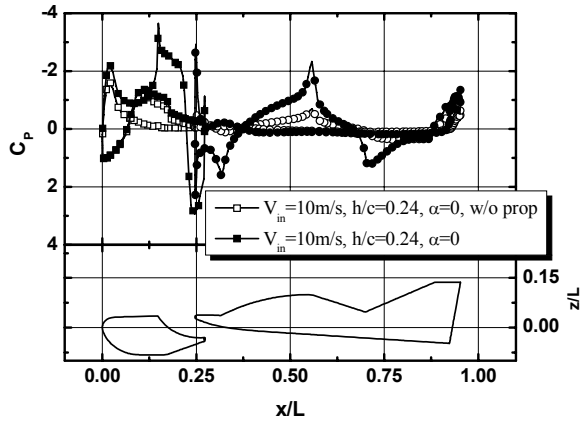

(b) C_P at low pitch angle ; $\alpha = 0^o$

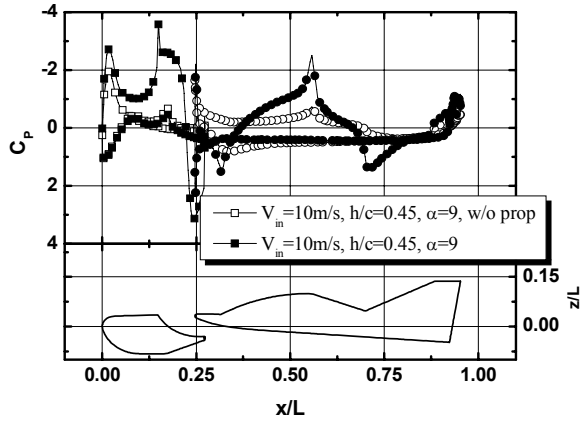

(c) C_P at $h/c = 0.45$ and $\alpha = 9^o$

Fig. 10. Comparison of pressure distributions.

difference causes the aerodynamic characteristics to change as discussed in Figs. 5 (lift), 6 (lift-drag), and 7 (moment). On the other hand, the C_p along the lower surface has almost the same values for the two cases. The propeller is located at 25% from the fore part of the fuselage as can be seen in the lower part of Fig. 10 so that a sharp increase in the pressure can be observed at $x/L = 0.25$ for the case of with DUP. It is also found that the pressure distribution on the upper surface for DUP is not varied with the vehicle's heights (i.e., Fig. 10(a) and (c)) and pitch angles (see Fig. 10(a) and (b)). Generally, the influxed air between the fuselage and the ground tends to stagnate, changes from dynamic pressure to static pressure in the chamber, and results in high pressure on the lower surface for a general WIG vehicle (i.e., without DUP device). However, for the case with DUP, an additional air chamber exists, such as a channel in the middle of the fuselage, so that the accelerated air flow by the propeller augments the amount of incoming flow through the fore gap by lowering the pressure under the fuselage, resulting in an increase in suction at $h/c = 0.24$ and $\alpha = 0^o$, as shown in Fig. 10(b).

The pressure distribution of lower surface plays an important role in the aerodynamic characteristics of a WIG vehicle with DUP device. It can be seen in Fig. 10 that the pressure distribution on the lower surface of fuselage is influenced by height (h/c) and pitch angle (α) due to the stagnation of accelerated air. When the accelerated air is properly stagnated in the air chamber, the pressure tends to increase gradually at the aft fuselage as shown in Fig. 10(a). When the vehicle is sufficiently close to the ground ($h/c = 0.24$) and has a large pitch angle ($\alpha = 9^o$) as shown in Fig. 10(a), the accelerated air by the DUP is stagnated in the air chamber and may improve the lift force dramatically, as discussed in Fig. 5. This is due to the fact that a considerable pressure change occurs owing to an increase in dynamic pressure through the propeller (at near $x/L = 0.25$). In addition, it is clear that the friction and pressure drags and the moment are also increased by a high dynamic pressure so that the largest lift but the smallest lift-drag ratio can be observed (see Fig. 6). Fig. 10(b), which has the same height ($h/c = 0.24$) as Fig. 10(a) but has a zero pitch angle, can explain the reason of a relatively low increase in lift at $\alpha = 0^o$ because of a high suction between the lower surface of fore body and ground as discussed in Fig. 5. However, an increase in drag by high dynamic pressure on the upper surface is expected. Yet, for the case of $h/c = 0.45$ and $\alpha = 9^o$ (Fig. 10(c)), it is hard to expect an increase in lift by DUP because of its large gap between the lower surface and ground.

Fig. 11 presents the pressure distributions along the center of the fuselage at $v_{in} = 10$ m/s and $\alpha = 9^o$ for different heights ($h/c = 0.24$ and 0.45) to explain the effect of height on the case with DUP. It is easily found that the pressure distributions on the upper surface of the WIG the vehicle show a simi lar trend irrespective of height because the effect of DUP on flow fields is dominant. An increase in lift, in general, mainly comes from the pressure augmentation on the lower surface of the WIG vehicle. It is expected that the drag is not considerably increased as the vehicle approaches the ground. For example, the friction drag for $h/c = 0.45$ is calculated as 0.62 and the value of that for $h/c = 0.24$ is 0.50. Even though the induced drag cannot be separated from the pressure drag, it is decreased with lower heights. The total drag is increased as the height is decreased because of the direction of the pressure exerting on the surface. The pressure on the lower surface becomes higher at the aft body for $h/c = 0.24$ while it is nearly constant at $h/c = 0.45$. How-

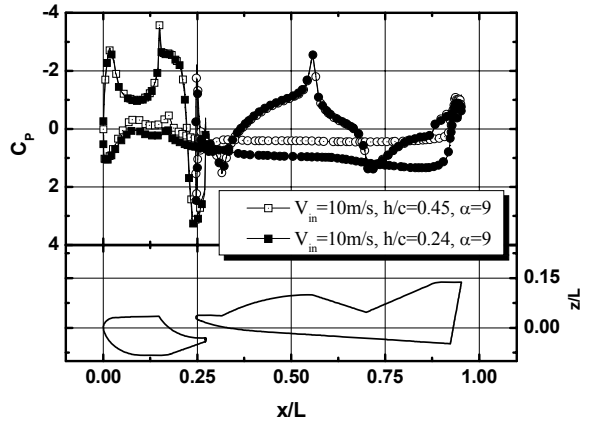

Fig. 11. DUP and ground effect with respect to height.

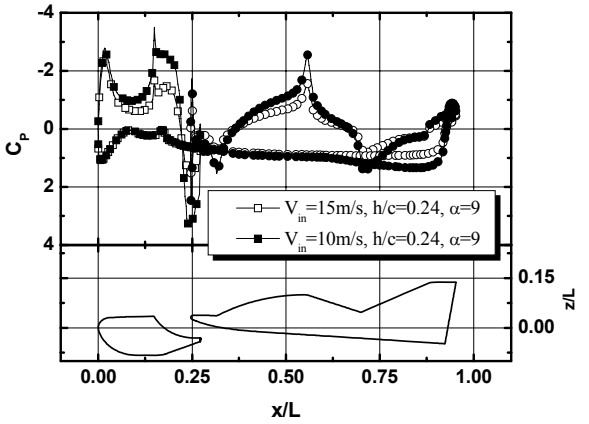

(a) C_P at high pitch angle ; $\alpha = 9^o$

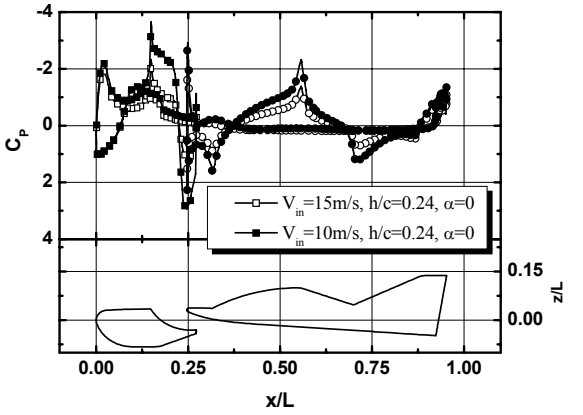

(b) C_P at low pitch angle ; $\alpha = 0^o$

Fig. 12. Effect of free stream velocity.

ever, the Venturi effect does not appear because of the high pitch angle ($\alpha = 9^o$) and this phenomenon agrees well with the general ground effect. To utilize the ground effect when it cruises, the vehicle used in this study holds a high pitching angle.

In order to explain the effect of cruise speed on the aerodynamic performance, the pressure distributions for $v_{in} = 10$ m/s and 15 m/s at $h/c = 0.24$ for various pitch angles ($\alpha = 9^o$ and 0^o) are plotted in Fig. 12. As shown in Fig. 12, the pressure on the upper surface depends on exit velocity of the propeller so that the difference between the two can be observed. The absolute value of the pressure of $v_{in} = 15$ m/s is higher, and nevertheless the pressure coefficient is smaller since the rate of the DUP (propeller) against dynamic pressure is small. Therefore, the results of drag polar for $v_{in} = 15$ m/s are placed on the left side of that for $v_{in} = 10$ m/s, as shown in Fig. 6. In Fig. 12(b), it is noteworthy that both pressure distributions on the lower surface are identical. It can be said that when both the angle of attack and the height are high for the case without ground effect, the flow on the lower surface mostly comes from the free stream (i.e. flow from DUP is not stagnated properly).

When the WIG vehicle with low pitch angle ($\alpha = 0^o$) is close to the ground ($h/c = 0.24$), as shown in Fig. 13(a) and (b), the Venturi effect and a pressure recovery on the lower surface of the fore body with suction on the upper surface are observed. This increase in pressure at the fore part of the fuselage results in a nose-up moment and a positive moment. The relatively significant moment changes can be seen in Fig. 13(a) for the vehicle without DUP. However, the pressure coefficient at the upper surface is not influenced by the angle of attack for the vehicle with DUP. As discussed in Fig. 7, it is expected that the changes of the pitching moment with respect to the height are small. Zerihan and Zhang [32], who performed the experiment for inverse-cambered wing, also showed a pressure recovery on the lower surface at $\alpha = 0^o$. Although Zerihan and Zhang did not explicitly explain the reasons for the pressure increment at the lowest height, the obvious pressure recovery before the minimum gap could be seen in pressure distributions on the lower surface. Ahmed and Sharma [24] also showed the pressure increment at the lowest ground gap. This pressure increment is different from that of a general ground effect vehicle which leads to high pressure at the aft part of the wing by stagnation of oncoming air. It is said that the air coming to the lower surface could not go through the gap between maximum thickness of the wing and ground because of the boundary layers on the ground and wing surface. Thus, the air was stagnated on the leading edge and it leads to high pressure on the same surface.

3.3 Pressure distributions on the lower surface

As shown in previous explanations, the pressure on the lower surface increases as the gap between the vehicle and the ground gets smaller, and it improves aerodynamic performance. This is due to the fact that the pressure with a small gap becomes high because air is stagnated properly, whereas air in Fig. 14(b) can escape. In addition, the pressure for the case with DUP (Fig. 14(a)) becomes much higher than that without DUP (Fig. 14(c)) at the same height and pitch angle (i.e., $h/c = 0.24$ and $\alpha = 9^o$). The pressure on the aft portion of the fuselage increases because of additional air flow coming through the DUP. It is also shown that the pressure distribution for the case with DUP in Fig. 14(a) becomes asymmetric because of the rotational component whereas the pressure for the case without

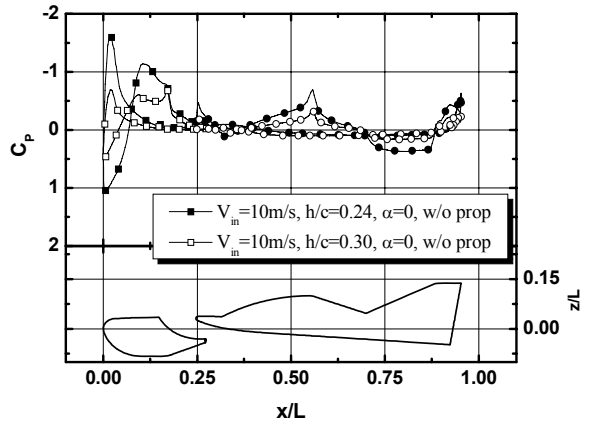

(a) C_P without DUP

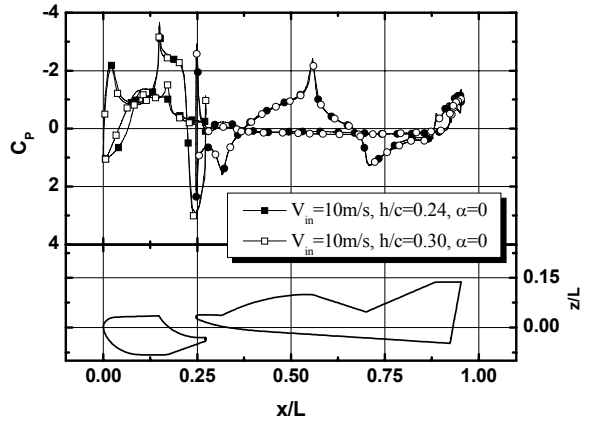

(b) C_P with DUP

Fig. 13. Variation of C_p distributions at fore part of the fuselage with respect to height.

DUP becomes symmetric. It clearly shows that the DUP produces a negative pitching moment and this negative moment leads to the unfavorable for height stability of DUP.

4. Conclusions

A 3-dimensional numerical investigation of the WIG effect vehicle with DUP was performed and aerodynamic characteristics and static height stability were analyzed. A WIG effect vehicle with all compartments such as propeller, fuselage, air chamber, main wing, and tail was considered. The DUP with increased pressure in the air chamber can considerably reduce take-off speed and thus minimize the effect of the hump drag while the vehicle accelerates to take off on water. However, it also increases the drag by high dynamic pressure on the entire surface of the vehicle and stunts high performance.

The computational results clearly show that the DUP can dramatically improve lift but is not favorable for aerodynamic performance and stability. The air with high energy through the DUP slows down and turns its energy to lift in the air chamber under the fuselage. When the vehicle is in ground effect such as $h/c < 0.35$ and $\alpha > 3^{o}$, stagnation of the air results in high pressure at the aft part of the air chamber, generating sufficient lift. However, the high pressure naturally leads to a negative pitching moment and moves X_h downstream. The closer the height of the vehicle is to the ground, the higher the pressure is.

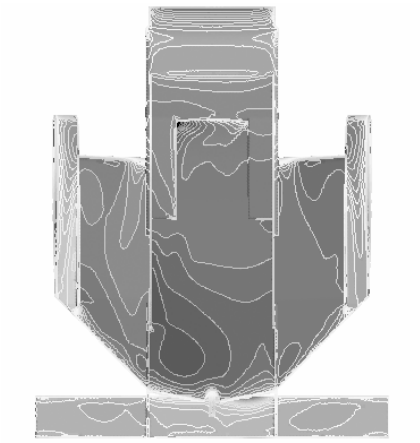

(a) h/c = 0.24, $\alpha = 9^{o}$ for with DUP

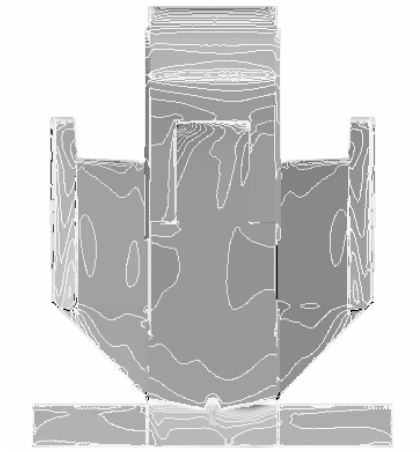

(b) h/c = 0.45, $\alpha = 9^{o}$ for with DUP

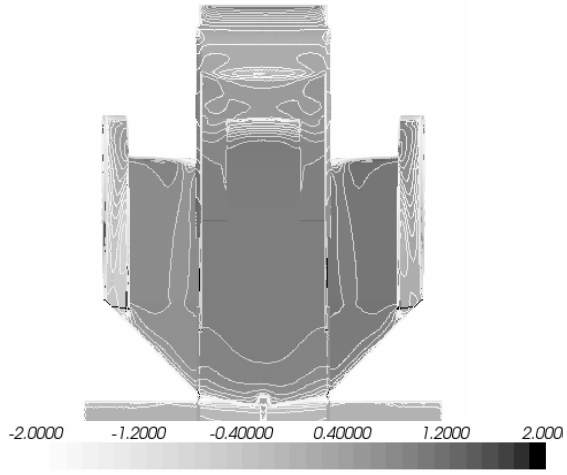

(c) h/c = 0.24, $\alpha = 9^{o}$ without DUP

Fig. 14. Pressure coefficient distributions on the lower surface.

As a result, this is one of the major factors for aggravating the *H. S.* It is also necessary that designers for WIG effect vehicles be careful in designing the DUP to enhance takeoff.

Acknowledgment

This research was supported by the Academic Research fund of Hoseo University in 2007-0129.

Nomenclature

A	: Wing area
AR	: Aspect ratio (A/c^2)
c	: Chord length
C_D	: Drag coefficient($D/0.5\rho v_{in}^2 A$)
C_L	: Lift coefficient ($L/0.5\rho v_{in}^2 A$)
C_P	: Pressure coefficient
C_{MP} , C_M	: Pitching moment coefficient
C_{MR}	: Rolling moment coefficient
D	: Drag
H. S.	: Static height stability in Eq. (5)
h	: Height of vehicle
L	: Lift
Re	: Reynolds number
v_{in}	: Free stream velocity
X_h	: Aerodynamic center of height
X_α	: Aerodynamic center of pitch angle
α	: Pitch angle
ρ	: Density of air

References

[1] C. Wieselsberger, *Wing resistance near the ground*, NACA TM77 (1922).

[2] M. P. Fink and J. L. Lastinger, *Aerodynamic characteristics of low-aspect-ratio wings in close proximity to the ground*, NASA TN D-926 (1961).

[3] A. W. Carter, *Effect of ground proximity on the aerodynamic characteristics of aspect-ratio-1 airfoils with and without end plate*, NASA TN D-970 (1961).

[4] K. H. Jung, H. H. Chun and H. J. Kim, Experimental investigation of wing-inground effect with a NACA6409 section, *Journal of Marine*, 13 (3) (2008) 317-327.

[5] K. W. Park and J. H. Lee, Influence of endplate on aerodynamic characteristics of low aspect ratio wing in ground effect, *J. of Mechanical Science and Technology*, 22 (12) (2008) 2578-2589.

[6] K. W. Park and J. H. Lee, Optimal design of two-dimensional wings in ground effect using multi-objective genetic algorithm, *Ocean Engineering*, 37 (2010) 902-912.

[7] K. V. Rozhdestvensky, Wing-in-gground effect vehicles, *Progress in Aerospace Sciences*, 42 (2006) 211-283.

[8] Wingship investigation, Volume 1, ARPA report (1994).

[9] M. R. Ahmed, T. Takasaki and Y. Kohama, Aerodynamics of a NACA4412 airfoil in ground effect, *AIAA Journal*, 45 (1) (2007) 37-47.

[10] R. W. Staufenbiel and U.-J. Schlichting, Stability of airplanes in ground effect, *Journal of Aircraft,* 25 (4) (1988) 289-294.

[11] R. Staufenbiel, Some nonlinear effects in stability and control of wing-in-ground effect vehicles, *Journal of Aircraft,* 15 (8) (1978) 541-544.

[12] N. Kornev and K. Matveev, *Complex numerical modeling of dynamics and crashes of wing-in-ground vehicles*, AIAA 2003-600 (2003).

[13] J. L. Thomas, J. W. Paulson and R. J. Margason, *Powered low-aspect-ratio wing in ground effect (WIG) aerodynamic characteristics*, NASA-TM-78793 (1979).

[14] M. Majji, R. Bhattacharya and J. L. Junkins, Dynamics and control of ground effect transportation system, *Proceedings of the 2007 American Control Conference*, New York City, USA (2007).

[15] H. H. Chun, J. H. Chang, K. J. Paik and M. S. Shin, Wind tunnel test on the aerodynamic characteristics of a PARWIG Craft, *Journal of the Society of Naval Architects of Korea*, 37 (3) (2000) 57-68.

[16] K. W. Park, J. B. Kim and J. H. Lee, Aerodynamic characteristics and static height stability of WIG effect vehicle with direct underside pressurization, *Trans. of the KSME (B)*, 33 (12) (2009) 961-967.

[17] J. H. Lee, B. S. Kim and K. W. Park, Flow characteristics of WIG-effect vehicle with direct-underside-pressurization system and propeller, *Trans. of KSME (B)*, 34 (6) (2010) 649-654.

[18] W. Rodi, Turbulence models and their applications in hydraulics-a state art of review, *Book Publication of International Association for Hydraulic Research*, Delft, Netherlands (1984).

[19] STAR-CCM+ v4.02, Methodology, *Computational Dynamics, Co.*, London. U. K. (2008).

[20] S. V. Patankar, Numerical heat transfer and fluid flow, *McGraw-Hill Book Company*, New York (1980).

[21] K. W. McAlister and R. K. Takahashi, *NACA 0015 Wing pressure and trailing vortex measurements*, NACA Technical Paper 3151 (1991).

[22] E. N. Jacobs and A. Sherman, *Airfoil section characteristics as affected by variations of the reynolds number*, NACA TM586 (1939).

[23] J. D. Anderson, *Aircraft performance and design*, McGraw-Hill (1999).

[24] M. R. Ahmed and S. D. Sharma, An investigation on the aerodynamics of a symmetrical airfoil in ground effect, *Experimental Thermal and Fluid Science*, 29 (2005) 633-647.

[25] R. Ranzenbach and J. B. Barlow, Two-dimensional airfoil in ground effect, An Experimental and Computational Study, *1994 Motor Sports Engineering Conference* (1994) 241-250.

[26] Y. Moryoseff and Y. Levy, Computational study of the flow about an oscillating wing in ground effect, AIAA 2001-0863. *39th AIAA Aerospace Sciences Meeting & Exhibit*, Reno, USA (2001).

[27] J. Zerihan and X. Zhang, Aerodynamics of a single element wing in ground effect, AIAA2000-0650, *38th AIAA Aerospace Sciences Meeting and Exhibit*, Jan. 10-13, Reno, NV, USA (2000).

[28] X. Zhang and J. Zerihan, Edge vortices of double-element wing in ground effect, *Journal of Aircraft*, 41 (5) (2004) 1127-1137.
[29] R. C. Nelson, *Flight stability and automatic control,* McGraw-Hill (1998) 42-44.
[30] M. Halloran and S. O'Meara, *Wing in ground effect craft review*, DSTO-GD-0201, 1999.
[31] R. D. Irodov, Criteria of longitudinal stability of ekranoplan, *Ucheniye Zapiski TSAGI*, 1 (4) (1970) 63-74.
[32] J. Zerihan and X. Zhang, Aerodynamics of gurney flaps on a wing in ground effect, *AIAA Journal*, 39 (5) (2001) 772-780.

Kyoungwoo Park is currently working at Department of Mechanical Engineering of Hoseo University as a Professor. He has received BA degree in 1985, MA degree in 1990, and Ph.D degree in 1995, respectively, at the department of mechanical engineering of Hanyang University, Seoul, Korea. As soon as he acquired his Ph.D. degree, he entered the LG Industrial Systems Co., Ltd., and researched on the flow and thermal characteristics around/in elevators. In 1999, he joined the Ralph Greif research team for two and half years, who is a professor of University of California at Berkeley, and studied convection heat transfer with CFD. After he came back to Korea in 2001, he researched and taught at Hanyang University until Feb. 2005. His main interesting fields are heat transfer, micro/macro thermo/fluid dynamics, optimization, and CFD. Recently, his researches are focused on the semiconductor and display manufacturing process and the aerodynamics and optimization of Wing-In-Ground effect vehicles.

Byungmoon Kim is currently working at the Department of Energy & Environmental Systems of Dongguk University as a professor. He received his Ph.D in 1999 at the Department of Heat-Energy System Engineering of Kyushu University, Japan. He researched the in-situ analysis of nano-structured WC-Co feedstock and coating properties via HVOF process at RIST from 2000 until 2003. He worked with the government agency chief of the KEMCO new and renewable energy center which is a government authority which gives new and renewable energy policy inventory, certification, PRS, RFS, 1 million green homes, loan/tax incentive and an international cooperation from 2008 until 2010. His main interesting fields are plasma coating, jet nozzle design, particles flow, wind power design and battery re-manufacture.

Juhee Lee received his Ph.D in 2006 on "Pareto optimization of WIG airfoil based on the multi-objective genetic algorithm" from Hanyang University. After working at a CFD engineering company for 5 years as a senior engineer, he is currently working at the Hoseo University as a lecturer since 2007. His major topics of interest covers WIG design, aircraft performances, fluid dynamics, numerical methods, and multi-objective optimization.